BIOCHEMICAL PHARMACOLOGY 76 (2008) 1669–1680

available at www.sciencedirect.com

ScienceDirect

journal homepage: www.elsevier.com/locate/biochempharm

Kinetic stabilization of microtubule dynamic instability by benomyl increases the nuclear transport of p53

Krishnan Rathinasamy, Dulal Panda *

School of Biosciences and Bioengineering, Indian Institute of Technology Bombay, Powai, Mumbai 400076, India

ARTICLE INFO

Article history:
Received 11 August 2008
Accepted 2 September 2008

Keywords:
Benomyl
Dynamic instability
Mitosis
Nuclear transport
p53

ABSTRACT

Using time-lapse confocal microscopy and enhanced green fluorescent protein–tubulin transfected MCF-7 cells, we found that a tubulin-targeted antimitotic agent, benomyl at its half-maximal proliferation inhibitory concentration (5 μM) strongly suppressed the rate and extent of growing and shortening excursions of individual microtubules in MCF-7 cells without noticeably depolymerizing the microtubule network or decreasing the polymerized mass of tubulin. Further, benomyl treatment caused an increase in the acetylation level of microtubules suggesting that it stabilizes microtubules. Under the conditions that suppressed the dynamic instability, a sharp increase in the nuclear accumulation of p53 in MCF-7 cells was observed in the presence of benomyl. Up regulation of bax and the increased nuclear accumulation of p21 upon benomyl treatment confirmed the activation of p53. Cisplatin caused an increase in the translocation of p53 into the nucleus in the presence of lower effective concentrations of benomyl while a decrease in the nuclear accumulation of p53 was observed in the presence of high concentrations of benomyl suggesting that the stabilized microtubules assist in the nuclear transportation of p53. Furthermore, increased localization of the light chain of the minus end directed motor protein dynein was detected on the microtubules in the benomyl-treated cells indicating that the suppression of microtubule dynamics may influence the binding of dynein on the microtubules and dynein-mediated cargo transport. Together the data indicate that benomyl inhibits mitosis primarily by suppressing the dynamic instability of microtubules and support the hypothesis that the kinetic stabilization of microtubules enhances the microtubule-mediated transport of p53 into the nucleus.

1. Introduction

Benomyl, a benzimidazole systemic agricultural pesticide, is extensively used against a range of fungal diseases [1]. It is known to exert selective toxicity against fungal cells due to its higher affinity for fungal tubulin than mammalian tubulin [2]. It has been shown to have a very low acute systemic toxicity (LD_{50} greater than 10 g/kg) in rats [3]. Tubulin is believed to be the target of benomyl in yeast cells based on specific mutation studies in the β tubulin gene, which altered the resistance or sensitivity of yeast cells to benomyl [4–6]. Benomyl was thought to bind at or near the colchicine binding site based on their structural similarities and the fact that several members of the benzimidazole group of compounds inhibit the binding of colchicine to tubulin both competitively and noncompetitively [6–8]. However, recent studies have suggested that

* *Corresponding author*. Tel.: +91 2225767838; fax: +91 2225723480.
E-mail address: panda@iitb.ac.in (D. Panda).

Abbreviations: IC_{50}, half-maximal inhibitory concentration; DAPI, 4′,6-diamidino-2-phenylindole; SRB, sulforhodamine B; DLC, dynein light chain; ALP, alkaline phosphatase; BCIP, Bromo-Chloro-Indolyl-Phosphate; NBT, Nitro Blue Tetrazolium.

0006-2952/$ – see front matter © 2008 Elsevier Inc. All rights reserved.
doi:10.1016/j.bcp.2008.09.001

benomyl and colchicine bind at distinct sites on tubulin [9,10]. Benomyl was shown not to inhibit the binding of colchicine to mammalian tubulin and it was also found to bind to the tubulin–colchicine complex [10]. Benomyl is quite unstable and it decomposes in aqueous solutions into more stable compounds like carbendazim, and *N*,*N*′-dibutyl urea [11,12]. Carbendazim is the functionally active metabolite, which is believed to have similar actions as benomyl [1,6,13,14]. The conversion of benomyl to carbendazim is slow in aqueous environment and it could take several days [11,12].

Benomyl inhibits the proliferation of fungal [1,6] and mammalian cells by arresting the cells at mitosis [10,15]. Benomyl has been shown to bind to mammalian tubulin with a modest affinity and to inhibit the polymerization of brain microtubules *in vitro* [10]. In addition, benomyl has been shown to suppress the dynamic instability of bovine brain microtubules *in vitro* and the assembly of cold-depolymerized spindle microtubules in HeLa cells [10,15]. Previous reports have shown that benomyl at its half-maximal inhibitory concentration (IC_{50}) did not significantly depolymerize the interphase microtubules, however, inhibited mitosis in HeLa cells by perturbing the microtubule–kinetochore interactions and activating the mitotic checkpoint protein BubR1 [10,15].

Microtubules are highly dynamic polymers composed of α and β tubulin heterodimers. It is now well established that the polymerization dynamics of microtubules play critical roles in orchestrating several functions of microtubules [9,16–18]. Microtubules are the targets for various successful anticancer drugs like vincristine, vinblastine, paclitaxel and several other drugs like epothilone, estramustine, and noscapine, which are in different stages of clinical trials [18–20]. Microtubule targeted agents have also been shown to alter the expression [21] and translocation of the tumor suppressor protein, p53 into the nucleus [22,23] suggesting that the nuclear accumulation of p53 is linked with the assembly dynamics of microtubules. Further, the translocation of p53 into the nucleus is thought to occur through the microtubule tracks [22–24] and low concentration of microtubule targeted drugs is shown to increase the nuclear accumulation of p53 [22].

Recently, the antifungal drug griseofulvin is gaining importance because of its low toxicity and its ability to inhibit the proliferation of cancer cells similar to other potential anticancer drugs [25–27]. Rebacz et al. have shown that griseofulvin specifically targeted tumor cells and inhibited their proliferation without having much effect on normal cells [27]. In addition, carbendazim the active metabolite of benomyl [1,13,14], is presently undergoing clinical trials for the treatment of advanced solid tumors (ClinicalTrials.gov Identifier: NCT00023816, NCT00003709); hence, understanding the mechanism of action of benomyl is also of clinical importance.

In this study, we provide evidence suggesting that benomyl inhibited cell proliferation at mitosis by suppressing the dynamic instability of microtubules. Benomyl treatment increased the acetylation level of microtubules and also caused an increase in the localization of dynein light chain (DLC) on microtubules. In addition, the suppression of microtubule dynamics by benomyl was found to be associated with an increase in the nuclear accumulation of p53. The data presented in this study suggested that the suppression of microtubule dynamics by a small molecule may have a wide range of cellular effects including the perturbation of cargo transport through microtubule tracks. The results indicated that the combined use of an inhibitor of microtubule dynamics and a p53-activating agent may have significant advantage in cancer chemotherapy.

2. Materials and methods

2.1. Materials

Benomyl was purchased from Sigma–Aldrich (Milwaukee, WI, USA), paclitaxel, sulforhodamine B (SRB), mouse monoclonal anti α tubulin IgG, mouse monoclonal anti β tubulin IgG, anti acetyl tubulin IgG, alkaline phosphatase (ALP) conjugated anti mouse IgG, ALP conjugated anti rabbit IgG, bovine serum albumin (BSA), 4′,6-diamidino-2-phenylindole (DAPI) and G418 were purchased from Sigma (St. Louis, MO, USA). Rabbit polyclonal anti human bax was purchased from BD Pharmingen (San Diego, CA, USA). Mouse monoclonal anti DLC IgG was a gift from Dr. Krishanu Ray (TIFR, Mumbai). Anti mouse IgG-alexa 568 conjugate was purchased from Molecular Probes (Eugene, OR, USA). Mouse monoclonal anti p53 IgG, and mouse monoclonal anti p21 IgG, Annexin V apoptosis detection Kit were purchased from Santa Cruz Biotechnology (CA, USA). All other reagents used were of analytical grade.

2.2. Cell culture, cell proliferation assay and transfection

MCF-7 cell line was obtained from the National Centre for Cell Science, Pune. MCF-7 cells were grown in minimal essential medium (Hi Media, Mumbai) supplemented with 10% (v/v) fetal bovine serum, 0.3 IU/mL biosynthetic human insulin (Novo Nordisk, India Private Ltd.) and sodium bicarbonate (1.5 mg/mL) in the presence of antibiotics at 37 °C in a humidified atmosphere of 5% CO_2 and 95% air [15]. The effects of benomyl on MCF-7 cell proliferation were determined in 96-well tissue culture plates by the standard SRB assay [15,28]. Benomyl stock solutions were freshly prepared in 100% dimethyl sulfoxide (DMSO); the final DMSO concentration in all experiments was 0.1%. DMSO (0.1%) alone was used as a vehicle control in all experiments. Enhanced green fluorescent protein (EGFP)-α tubulin plasmid was a kind gift from Dr. Leslie Wilson (University of California, Santa Barbara). EGFP-α tubulin plasmid was amplified in *Escherichia coli* XL1 Blue cells and isolated using Qiagen endotoxin free plasmid isolation kit (Qiagen GmbH, Hilden, Germany) according to the manufacturer's instructions. Transfection of MCF-7 cells was carried out by electroporation using a Gene Pulser Xcell (Bio-Rad, USA). Cells stably expressing EGFP-α tubulin were selected using G418 (Sigma) and maintained in the cell culture media containing G418 [20].

The mitotic index was calculated by counting the number of mitotic and interphase cells after staining the chromosomes with DAPI as described earlier [15]. The mitotic and interphase cells were counted under the Eclipse TE-2000 U microscope (Nikon, Kanagawa, Japan). At least 600 cells were scored for each concentration of benomyl and the experiment was repeated four times.

2.3. Immuofluorescence microscopy

MCF-7 cells were seeded on glass coverslips at a density of 6×10^4 cells/mL in 24-well tissue culture plates. After 24 h the old media were replaced with fresh media containing different concentrations of benomyl and incubated for further 24 h. Cells were then fixed in 3.7% formaldehyde at 37 °C and then immunofluorescently labeled as described earlier [15,26] to visualize tubulin, p53 or p21. DNA was stained with DAPI. To visualize both tubulin and acetyl tubulin, MCF-7 cells stably expressing EGFP-α tubulin were grown on coverslips and processed for immunofluorescence microscopy using mouse monoclonal anti acetylated α tubulin IgG and anti mouse IgG-Alexa-568 conjugate. The total intensity per unit area of tubulin fluorescence and acetylated tubulin fluorescence of different cells were calculated using Image-Pro Plus software (Media Cybernetics, Silver Spring, MD, USA). To visualize both tubulin and DLC, MCF-7 cells stably expressing EGFP-α tubulin were grown on coverslips and processed for immunofluorescence microscopy using mouse monoclonal anti DLC IgG (1:300 dilutions) and anti mouse IgG-Alexa-568 conjugate (1:400 dilutions). The coverslips were mounted in 80% glycerol in phosphate buffered saline (PBS) containing 1,4-diazabicyclo[2.2.2]octane (DABCO) and observed either with a Nikon Eclipse TE-2000 U microscope or a 60× water immersion objective in a FV 500 laser scanning confocal microscope (Olympus, Tokyo, Japan). The images were processed and analyzed using Image-Pro Plus software.

2.4. Annexin V/propidium iodide staining

Annexin V/propidium iodide staining of MCF-7 cells grown in the absence and presence of different concentrations of benomyl for 48 h was carried out as described previously [29]. The cells were stained using the Annexin V apoptosis detection kit (Santa Cruz Biotechnology, CA, USA) according to the manufacturer's protocol and processed for microscopy. The number of cells found positive for Annexin V and propidium iodide were counted under the microscope using the FITC and propidium iodide fluorescence, while the total cells were counted by observing the differential interference contrast images.

2.5. Measurement of microtubule dynamics

MCF-7 cells stably expressing EGFP-α tubulin were seeded on coverslips at a density of 6×10^4 cells/mL. The cells were then treated with vehicle or different concentrations of benomyl (3 and 5 μM) 48 h after seeding and incubated for further 24 h. The coverslips were then transferred to glass bottomed Petri dishes (Prime Bioscience, Singapore) containing the growth media without phenol red and maintained at 37 °C on a warm stage. The microtubules on the peripheral region of the MCF-7 cells were observed using a 60× water immersion objective in a FV 500 laser scanning confocal microscope (Olympus, Tokyo, Japan). The time lapse images were acquired at 2 or 4 s intervals for a total period of 120–180 s using the Fluoview sofware (Olympus, Tokyo, Japan). The lengths of the microtubules at different time points were calculated using Image-Pro Plus software. The dynamic instability parameters were calculated as described earlier [26].

2.6. Preparation of total cell lysate and fractions containing polymeric and monomeric (soluble) tubulin

MCF-7 cells were incubated with or without different concentrations of benomyl in tissue culture flasks. Both the floating and attached cells were harvested with the help of a cell scrapper and collected by centrifugation. The total cell lysates were collected as described earlier [15,30,31]. The cell lysates containing polymeric and soluble tubulin (monomeric tubulin) were prepared as described earlier [32,33]. Briefly, cells were collected, washed twice in PBS and then incubated at 37 °C with a microtubule stabilization buffer (0.1 M MES, pH 6.75, 1 mM $MgSO_4$, 2 mM EGTA, 4 M glycerol) containing 0.1% Triton X-100 for 10 min. The cells were centrifuged and the supernatant fraction containing the monomeric tubulin was separated from the cell pellet. The remaining cell pellets containing the polymeric tubulin were lysed in the lysis buffer containing protease inhibitors. The lysate, which was collected by centrifugation, was used as the polymeric fraction.

2.7. Western blot analysis

Protein concentration of the cell lysates was determined by Bradford assay [34] and samples containing equal amount of total protein were separated by SDS-PAGE and electro blotted onto a PVDF membrane (Hybond-P, Amersham). For determining the polymeric mass of tubulin and acetyl tubulin, the protein bands were probed using mouse monoclonal anti α tubulin IgG or mouse anti acetyl tubulin IgG. The ALP conjugated secondary antibodies were used at 1:5000 dilutions. The total intensity of the protein bands was calculated using Image-Pro Plus software. For analyzing p53 and bax, cell lysates equivalent to 35 μg of total protein were separated by SDS-PAGE (12% acrylamide gel) and electroblotted onto a PVDF membrane and probed with mouse anti p53 IgG and rabbit polyclonal anti human bax IgG. The secondary antibodies used were ALP-conjugated anti mouse and anti rabbit IgGs. The protein bands were visualized using Nitro Blue Tetrazolium/Bromo-Chloro-Indolyl-Phosphate (NBT/BCIP) substrate.

Cell lysates equivalent to 200 μg of total protein were immunoprecipitated with anti α tubulin IgG and protein A agarose beads [15]. The agarose beads were washed extensively and boiled with 2× SDS-PAGE sample buffer and loaded on 9% acrylamide gel. To cross link the interacting proteins the cell pellets were collected, washed in PBS and incubated with 1% (v/v) formaldehyde for 1 h at 37 °C [35]. Formaldehyde was removed and the cells were washed twice with PBS. The cells were then lysed with the lysis buffer in a tissue homogenizer (Hi Media, Mumbai). The cross linked proteins were subjected to immunoprecipitation with anti α tubulin IgG and agarose beads. To preserve the cross linking, the beads were incubated for 10 min at 37 °C with 2× SDS-PAGE sample buffer before loading on a 9% acrylamide gel [35,36]. The protein bands on the gel were electro blotted onto a PVDF membrane and probed with either anti α tubulin IgG or anti β tubulin IgG or anti p53 IgG.

3. Results

3.1. *Benomyl inhibits the proliferation of the MCF-7 cells without significantly altering the polymerized mass of microtubules*

Benomyl inhibited the proliferation of MCF-7 cells in a concentration dependent fashion with an IC_{50} value of about 5 ± 1 μM after 48 h of treatment (Fig. 1A). The inhibition of proliferation of MCF-7 cells was accompanied by cell cycle arrest at mitosis (Fig. 1A). At 5 μM benomyl treatment, ~16% of the cells were arrested at mitosis, while at 10 μM benomyl, ~36% of the cells were arrested at mitosis (Fig. 1A).

Western blot analysis of the polymeric tubulin fraction showed that benomyl (5 μM, IC_{50}) minimally (5%) decreased the polymeric mass of tubulin (Fig. 1B). However, higher concentrations of benomyl, such as 20 μM (4× IC_{50}) and 50 μM (10× IC_{50}) decreased the polymeric tubulin mass by 20% and 30%, respectively compared to the vehicle treated control cells. The quantification of monomeric tubulin amount in the soluble fraction of the cell extracts was in conformity with the reduction in polymerized amount of microtubules in the presence of benomyl (Fig. 1C). The amount of monomeric tubulin was found to increase by ~3%, 14% and 23%, in the presence of 5, 20 and 50 μM benomyl, respectively. Under similar conditions, 100 nM (10× IC_{50}) colchicine decreased the polymerized mass of microtubules by 63%.

Vehicle treated control cells exhibited well spread interphase microtubular network (Fig. 2A). The organization of the interphase microtubules in the presence of 5 μM (IC_{50}) benomyl was found to be similar to that of the control cells (Fig. 2A). The mitotic spindles of control MCF-7 cells were well organized with the chromosomes aligned compactly at the metaphase plate (Fig. 2B). In the presence of 5 μM benomyl, most of the mitotically arrested cells exhibited normal bipolar spindles; however, a few chromosomes were not aligned at the metaphase plate (Fig. 2B). Consistent with the Western blot analysis of the polymeric tubulin (Fig. 1B), 20 μM (4× IC_{50}) benomyl was found to induce a moderate depolymerization of the interphase microtubules (Fig. 2A). In the presence of 20 μM benomyl, most of the mitotically arrested cells had abnormal spindles and disorganized chromosomes (Fig. 2B). Cells treated with 50 μM benomyl exhibited significant depolymerization of both interphase and mitotic microtubules (Figs. 2A and B).

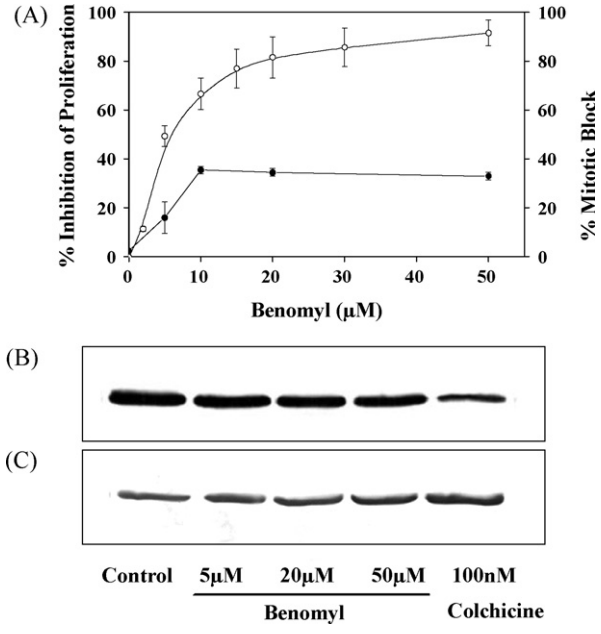

Fig. 1 – (A) Benomyl inhibited proliferation (○) and mitotic progression (●) in MCF-7 cells. Western blot analysis of the polymeric fraction of tubulin (B) and soluble (monomeric) tubulin (C) in the absence and presence of benomyl are shown. Polymeric and monomeric tubulin fractions were isolated as described in Section 2. Equal amounts of protein samples were resolved by SDS-PAGE followed by immunoblotting with anti α tubulin IgG.

3.2. *Benomyl treatment induced apoptotic cell death*

Control MCF-7 cells remained viable and healthy after 48 h as seen by the absence of Annexin V and propidium iodide staining. Benomyl-treated cells displayed a strong FITC-Annexin fluorescence and a very weak propidium iodide fluorescence indicating that the cells were in the early stages of apoptosis (Fig. 3A). Benomyl treatment increased the number of apoptotic cells in a concentration dependent fashion. For example, 2%, 9%, 24% and 38% of total cells were detected to be positive for FITC-Annexin fluorescence in the absence and presence of 5, 20 and 50 μM benomyl, respectively (Fig. 3B).

3.3. *Benomyl suppressed the dynamic instability of microtubules in living MCF-7 cells*

As reported earlier [20,37,38] control microtubules showed characteristic dynamic instability behavior. It was evident from the life history traces that benomyl potently suppressed the growing and shortening dynamics of individual microtubules in MCF-7 cells (Fig. 4). At the IC_{50} (5 μM), benomyl strongly suppressed the rates of growing and shortening of individual microtubules of MCF-7 cells by 38% (18 ± 3.6 μm/min to 11.2 ± 3 μm/min) and 47% (22 ± 6 μm/min to 11.6 ± 2.5 μm/min), respectively (Table 1). In addition, benomyl treatment reduced the mean growth length and shortening length of microtubules by 67% and 71%, respectively. The percentage of time the microtubules spent in growing and shortening states were decreased by 60% and 46%, respectively, while the percentage of time the microtubules spent in pause state was increased by 137%. It has been believed that catastrophe (a transition from a growing or a pause state to a shortening state) and rescue (a transition from a shortening state to a growing or a pause state) frequencies play important roles in regulating microtubule dynamics [39,40]. The time based rescue frequency (events/min) was found to be increased by 50% and the catastrophe frequency (events/min) was found to be decreased by 30% in the presence of 5 μM benomyl compared to the control cells. The length based rescue and the catastrophe frequencies (events/μm) were found to be increased by 180% and 225%, respectively, at the IC_{50} concentration of benomyl. The increase in the rescue

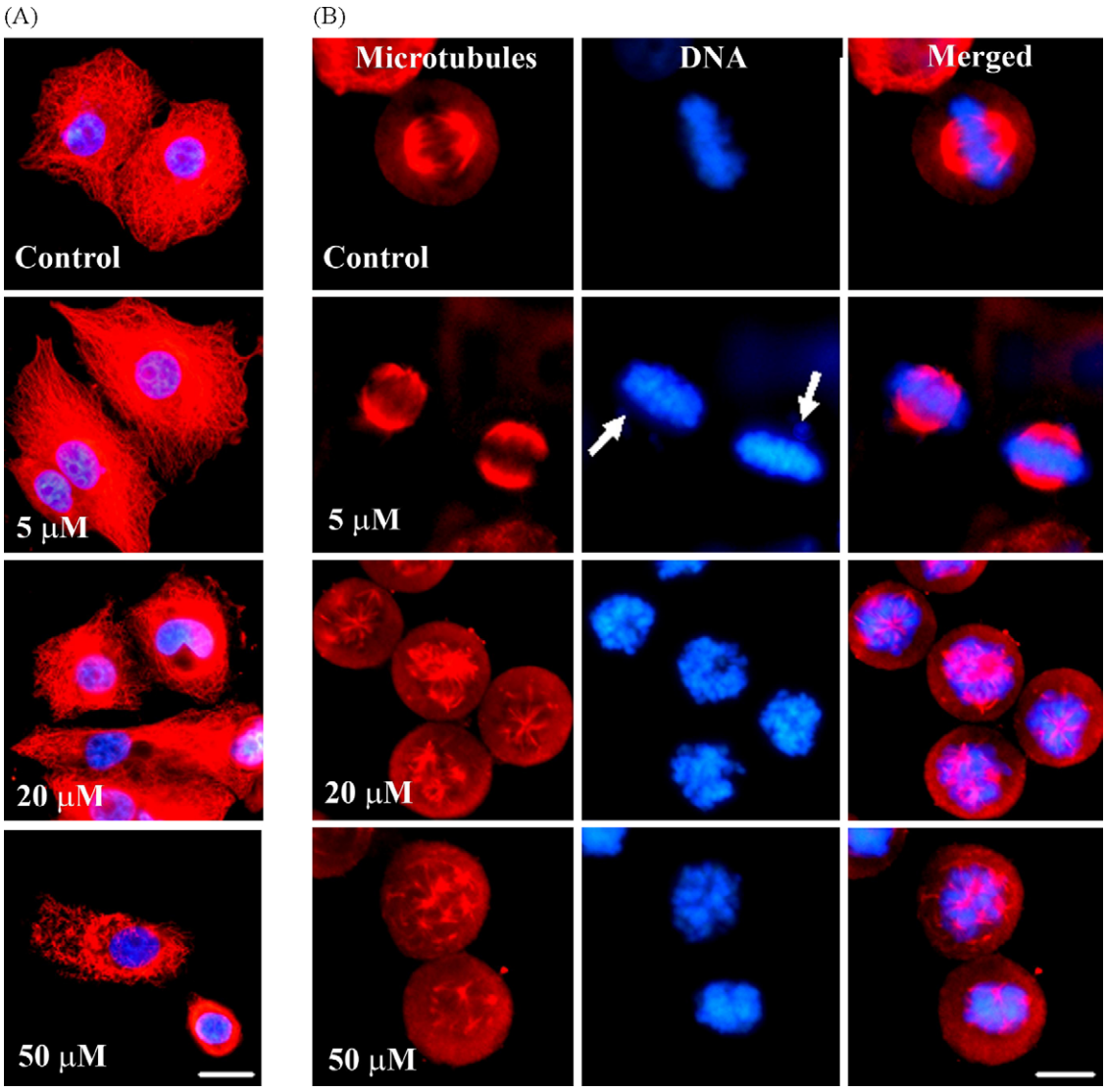

Fig. 2 – Effects of benomyl on the interphase and spindle microtubules and chromosome organization. MCF-7 cells were treated with the vehicle or the indicated concentration of benomyl for 24 h and processed to visualize microtubules and DNA. (A) Merged images of interphase microtubules and chromosomes are shown. Scale bar, 20 μm. (B) Organization of the spindle microtubules and chromosomes and the merged images are shown. Arrows indicate the misaligned chromosomes. Scale bar, 10 μm.

events/min and the decrease in the catastrophe events/min indicates that 5 μM benomyl inhibited depolymerization and initiated pause or growth state. The increase in the rescue and catastrophe events/μm implied that the growth and shortening length excursions of the treated cells were smaller than that of the control microtubules. The dynamicity (dimer exchange per unit time), which reflects the total length grown and shortened during the lifespan of the microtubules, was found to be suppressed by 74% in 5 μM benomyl-treated cells compared to that of the microtubules in control cells (Table 1).

The kinetic suppression of microtubule dynamics was also clearly discernible at lower concentration like 3 μM benomyl which caused significant suppression of the growth rate, shortening rate, growth length, shortening length of the microtubules. The overall dynamicity of the microtubules was decreased by ~50% in the presence of 3 μM benomyl.

3.4. *Benomyl treatment increased the acetylation of tubulin*

Acetylation of microtubules is considered as a marker for stabilized microtubules [38,41,42]. Since benomyl suppressed the dynamic instability of microtubules (Fig. 4 and Table 1), the acetylation status of tubulin in MCF-7 cells was analyzed after benomyl treatment. Benomyl treatment increased the acetylation of microtubules (Fig. 5A and B). The fluorescence intensities of EGFP microtubules and acetylated microtubules in MCF-7 cells were calculated using Image-Pro Plus software. The ratio of acetyl tubulin to total tubulin fluorescence was found to be increased by 2- and 3-fold in the presence of 5 and 20 μM benomyl, respectively, as compared to the vehicle treated MCF-7 cells. Western blot analysis of the polymeric tubulin fraction also indicated that benomyl treatment

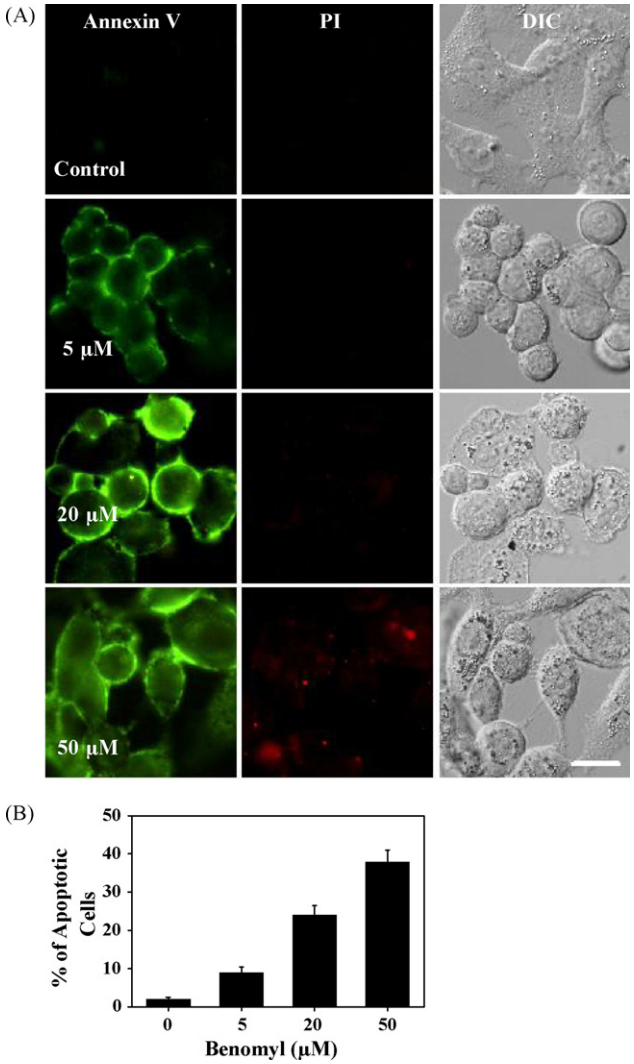

Fig. 3 – Benomyl induced apoptosis in MCF-7 cells. (A) MCF-7 cells were incubated with 0.1% DMSO (control) or different concentrations of benomyl for 48 h and then processed to visualize Annexin V, propidium iodide (PI) staining and differential interference contrast (DIC) images. Scale bar, 20 μm. (B) Percentage of apoptotic cells was plotted against benomyl concentration. Error bars are S.D..

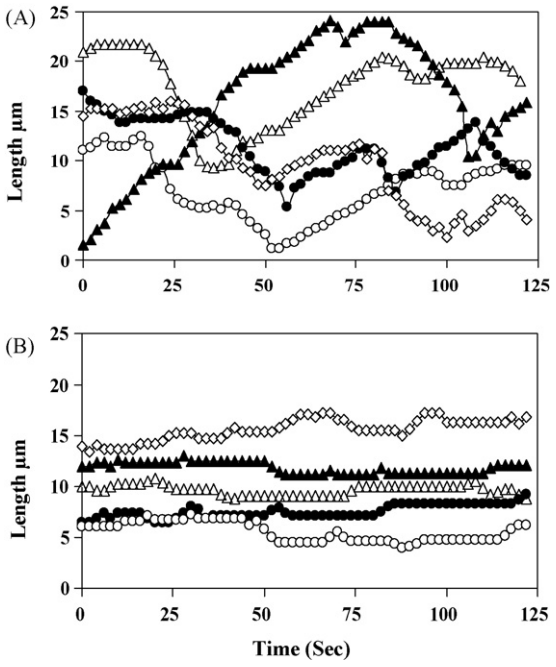

Fig. 4 – Benomyl suppressed the dynamic instability of individual microtubules of MCF-7 cells. Life history traces of individual microtubules of MCF-7 cells in the absence (A) and presence of 5 μM benomyl (B).

increased the acetylation level of tubulin (Fig. 5B). For example, the ratio of acetyl tubulin to tubulin in polymers was found to be increased by 30% and 70% in the presence of 5 and 20 μM benomyl, respectively.

3.5. *Benomyl increased the nuclear accumulation of p53 at the IC_{50} concentration*

The effects of benomyl on the expression and functions of p53 were analyzed in MCF-7 cells which have wild type functional p53. Cells were incubated in the absence or presence of benomyl for 24 h. In the vehicle treated MCF-7 cells, 2–4% of cells had p53 accumulated in the nucleus. Benomyl (5 μM) caused a strong increase in the expression of p53 in MCF-7 cells and >40% of the cells had p53 translocated into the

Table 1 – Effects of benomyl on the dynamic instability parameters of individual microtubules

	Benomyl (μM)		
	0	3	5
Rate (μm/min)			
Growing	18 ± 3.6	12.3 ± 2.8[a]	11.2 ± 3.0[a]
Shortening	22 ± 6	14.0 ± 4[a]	11.6 ± 2.5[a]
Length change (μm)			
Growth length	2.4 ± 1.2	0.9 ± 0.3[a]	0.8 ± 0.3[a]
Shortening length	2.8 ± 1.7	1 ± 0.2[a]	0.8 ± 0.2[a]
% Time in phase			
Growing	43.5 ± 15	33 ± 8[c]	17.4 ± 6[a]
Shortening	28 ± 11	24 ± 5[d]	15.0 ± 4[a]
Pause	28.5 ± 11	43 ± 10[a]	67.6 ± 9[a]
Frequency (events/min)			
Catastrophe	3.7 ± 2	4.90 ± 1.7[c]	2.6 ± 1.3[c]
Rescue	10 ± 6	15.4 ± 5[b]	15.0 ± 6[c]
Frequency (events/μm)			
Catastrophe	0.40 ± 0.3	1.0 ± 0.3[a]	1.3 ± 0.6[a]
Rescue	0.5 ± 0.5	2.2 ± 1[a]	1.4 ± 0.5[a]
Dynamicity (μm/min)	14.4 ± 4.3	7.1 ± 2[a]	3.8 ± 1.6[a]

Data are average ±S.D., $n = 30$ microtubules in control and $n = 20$ microtubules in 3 and 5 μM benomyl-treated cells.
[a] $P < 0.001$
[b] $P < 0.01$
[c] $P < 0.05$
[d] Statistically not significant.

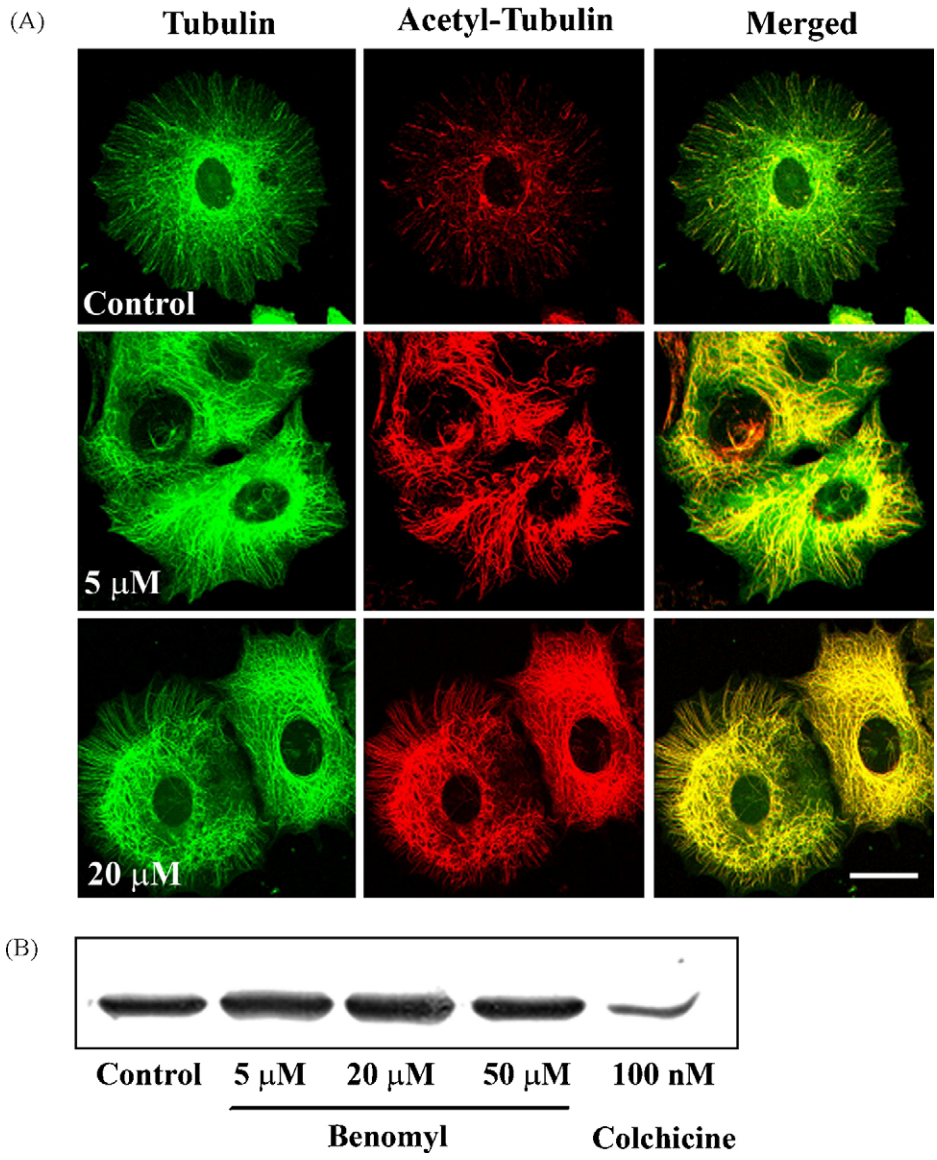

Fig. 5 – Effects of benomyl on the acetylation of tubulin. (A) EGFP-α tubulin transfected MCF-7 cells were treated with vehicle alone or different concentrations of benomyl (5 and 20 μM). Tubulin (green), acetylated tubulin (red), and the merged images are shown. Scale bar, 20 μm. (B) Western blot analysis of the polymeric acetyl tubulin of MCF-7 cells. The polymeric mass of acetylated tubulin was analyzed as described in Section 2.

nucleus (Fig. 6A). However, the translocation of p53 into the nucleus decreased with increasing concentration of benomyl. For example, with 50 μM benomyl treatment <6% of cells had p53 translocated into the nucleus (Fig. 6A).

The expression level of p53 was further analyzed by Western blotting (Fig. 6B). The expression level of p53 was found to increase by 9-, 7- and 5-fold when treated with 5, 20 and 50 μM benomyl, respectively, as compared to the control treatment. Although the expression level of p53 increased in the presence of 20 and 50 μM benomyl relative to control cells (Fig. 6B), the nuclear accumulation of p53 was inhibited under these conditions (Fig. 6A).

As reported earlier [43], treatment of the cells with the DNA damaging drug cisplatin increased the nuclear accumulation of p53 in MCF-7 cells (Fig. 6C). Low concentration (5 μM) of benomyl that potently suppressed the dynamic instability of microtubules enhanced the nuclear transportation of p53 into the nucleus of cisplatin treated cells. In contrast, depolymerizing concentration (50 μM) of benomyl inhibited the transport of p53 into the nucleus of cisplatin treated cells despite the overexpression of p53 as seen by the increased cytoplasmic p53 staining (Fig. 6C).

3.6. *Benomyl treatment caused overexpression of bax and nuclear accumulation of p21*

To confirm the activation of p53 by benomyl, the response of the downstream targets of p53 like p21 and bax were analyzed following benomyl treatment. The Western blot analysis with whole cell lysate of MCF-7 cells indicated that the proapoptotic protein bax was overexpressed upon benomyl treatment (Fig. 6B). For example, 5, 20 and 50 μM benomyl increased the

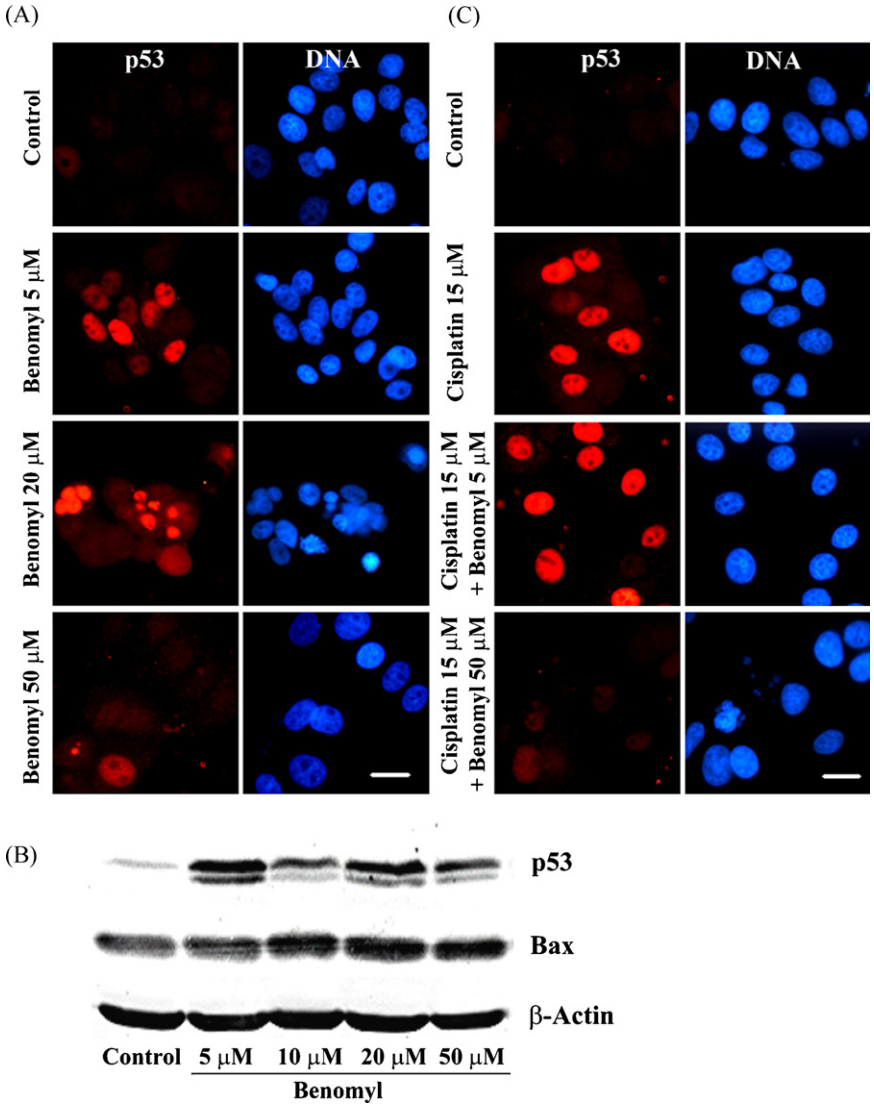

Fig. 6 – (A) Benomyl treatment increased the nuclear accumulation and activation of p53. MCF-7 cells were treated with different concentrations of benomyl for 24 h. Then, cells were fixed and processed to visualize p53 and DNA. Scale bar, 20 μm. (B) Benomyl increased the expression of p53 and its downstream protein bax in MCF-7 cells. MCF-7 cells were treated with DMSO (0.1%) (lane 1), 5, 10, 20 and 50 μM benomyl (lanes 2–5), for 24 h. Equal amounts of cell lysates as determined by using Bradford reagent were resolved by SDS-PAGE (12% acrylamide) followed by immunoblotting with anti p53 IgG, anti bax IgG and anti β actin IgG. (C) Depolymerization of microtubules by benomyl inhibited the nuclear accumulation of p53. MCF-7 cells were treated with vehicle, cisplatin alone or cisplatin in combination with benomyl for 24 h. Subsequently, cells were fixed and processed to visualize p53 and DNA. Scale bar, 20 μm.

expression of bax by 13 ± 6%, 30 ± 7% and 27 ± 4%, respectively. Benomyl treatment caused an increase in the nuclear accumulation of p21 in MCF-7 cells as observed by immunofluorescence microscopy (Fig. 7A). For example, ~4% of the vehicle treated cells showed nuclear accumulation of p21, while >50% of benomyl (5 μM) treated cells showed nuclear accumulation of p21.

3.7. *Benomyl treatment increased the binding of p53 to tubulin*

MCF-7 cells were treated with benomyl for 24 h and lysed without treatment or after treatment with formaldehyde. Tubulin from the cell lysates was immuno precipitated with anti α tubulin IgG and detected with anti p53 IgG by Western blotting. As reported earlier [24,44], p53 was found to be associated with microtubules in both the cells that were lysed without formaldehyde treatment (Fig. 7B, lanes 1–3) and after formaldehyde treatment for 1 h (Fig. 7B, lanes 4 and 5). In addition, 5 μM benomyl treatment was found to increase the binding of p53 to tubulin (Fig. 7B, lanes 4 and 5). To examine, whether p53 is associated only with either α or β tubulin subunit, the blots were probed separately with the monoclonal anti α and anti β tubulin IgGs. The tubulin–p53 complex was detected by all the three monoclonal antibodies (data not shown). The findings confirmed that p53 interacts with both

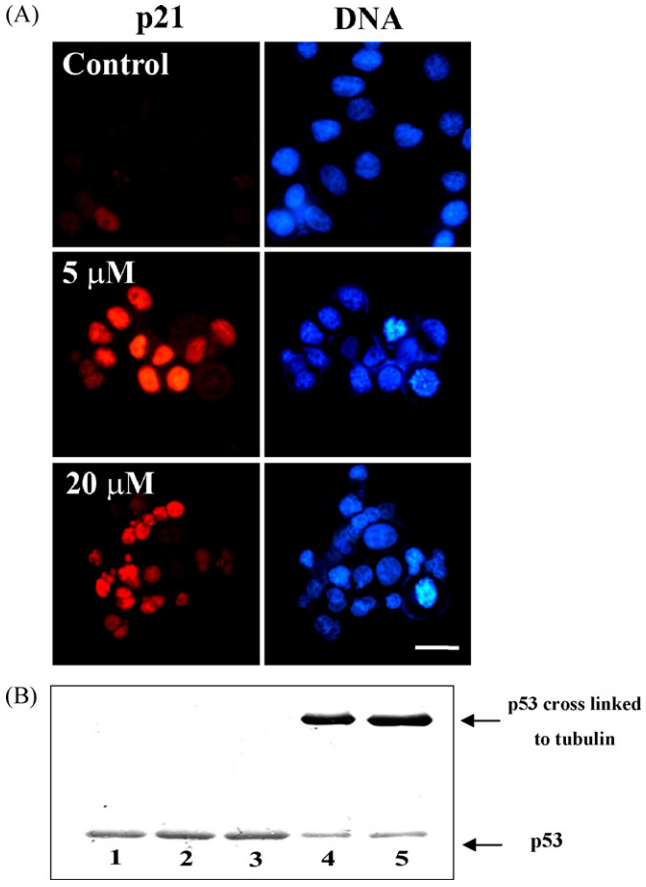

Fig. 7 – (A) Benomyl treatment increased the nuclear accumulation and activation of p21. MCF-7 cells were treated with benomyl (5 and 20 μM) for 24 h and then, fixed and processed to visualize p21 and DNA. Scale bar, 20 μm. (B) p53 protein is associated with microtubules in cells. Cell lysates equivalent to 200 μg of total protein were immunoprecipitated with anti α tubulin IgG, resolved by SDS-PAGE (9% gel), and immunoblotted onto a PVDF membrane and probed with anti p53 IgG. Lanes 1–3 correspond to the cell lysates of the control, 5 and 50 μM benomyl treatment, respectively. Lanes 4 and 5 correspond to the cell lysates of the control and 5 μM benomyl-treated cells that are cross linked before lysis and then immunoprecipitated with anti α tubulin IgG, and detected with anti p53 IgG.

tubulin in solution (dimers) and also microtubules in cells. All the antibodies used were specific and did not recognize other protein bands.

3.8. *Kinetic suppression of microtubule dynamics increased the association of DLC with microtubules*

Since p53 is reported to be transported into the nucleus through the microtubular tracks by the dynein/dynamitin motor complex [23,24], we examined the localization of the motor protein DLC on microtubules under normal conditions and under the suppressed dynamic instability conditions using EGFP transfected MCF-7 cells and confocal microscopy. In both the control and benomyl-treated cells, DLC was found to be co-localized with the microtubules (Fig. 8). In the control cells, DLC staining was observed to be diffused throughout the cells. In contrast, DLC staining was found to be more intense and finely localized along the length of the microtubules in the 5 μM benomyl-treated cells whose microtubules are kinetically stabilized than that of the control cells. Paclitaxel, an agent known to suppress the dynamics of microtubules [19] also exhibited a similar pattern of increased DLC staining in the peripheral microtubules.

4. Discussion

Benomyl was found to suppress the dynamic instability of the interphase microtubules in living MCF-7 cells. The increase in the acetylation level of tubulin in the benomyl-treated cells further suggested that the benomyl treatment kinetically stabilized the microtubules. Interestingly, a strong increase in the level of the dynein staining was observed on the microtubules of the benomyl-treated cells compared to that of the control cells suggesting that dynein binds to stabilized microtubules efficiently than the labile microtubules. Further, we provide evidence suggesting that the suppression of microtubule dynamics by benomyl facilitates the translocation of p53 into the nucleus.

Benomyl inhibited the proliferation of MCF-7 cells at mitosis and induced apoptotic cell death. Benomyl at its effective inhibitory concentrations strongly dampened the dynamics of microtubules in MCF-7 cells without significantly perturbing the organization of the microtubules or reducing the polymerized amount of tubulin. The data together suggest that benomyl inhibits mammalian cell proliferation at mitosis primarily by suppressing the dynamics of microtubules rather than depolymerizing them.

Benomyl caused a strong increase in the acetylation level of tubulin in MCF-7 cells (Figs. 5A and B). Stabilized microtubules are found to be acetylated in different cell types [38,41,42]. Considering that the acetylation of tubulin is a slow process compared to the growing and shortening rates at the microtubule ends, it was thought that the acetylation of tubulin requires stabilized microtubules [45]. Palazzo et al. have also observed that the acetylation of microtubules could be due to the stabilization of microtubules [46] and the acetylation per se may not enhance microtubule stability. Therefore, the increased acetylation of microtubules following benomyl treatment might be the consequence of the suppression of microtubule dynamics. Alternatively, the increased acetylation of tubulin could also be due to an inhibitory effect of benomyl on the histone deacetylase 6 (HDAC6), an enzyme that causes deacetylation of tubulin.

Low concentration (5 μM, IC_{50}) of benomyl increased the translocation of p53 into the nucleus, while, high concentration (50 μM) of benomyl inhibited the nuclear translocation of p53 into the nucleus suggesting that kinetically stabilized microtubules are required for the nuclear transport of p53. This was in conformity with the earlier report that high concentrations of microtubule interacting agents like paclitaxel, vincristine and nocodazole impaired the nuclear accumulation of p53 whereas low concentrations of these

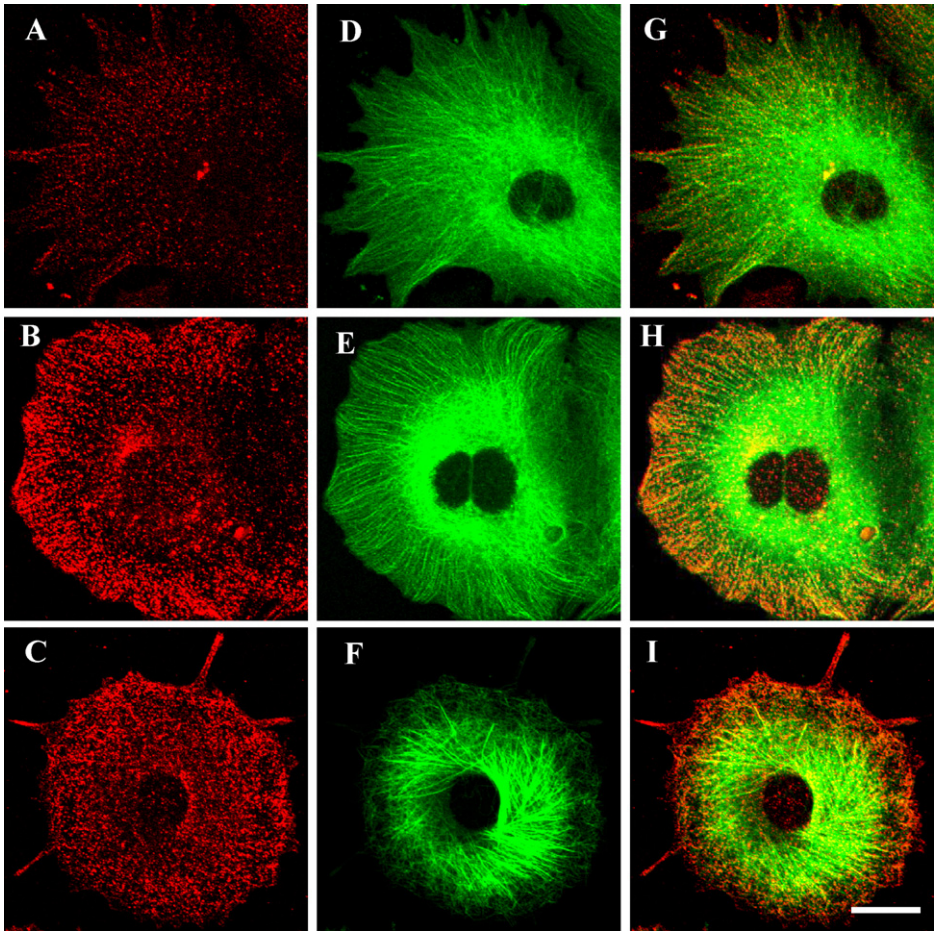

Fig. 8 – Suppression of microtubule dynamics increases the binding of DLC on the microtubules. EGFP-α tubulin transfected MCF-7 cells were treated with vehicle alone (A, D, and G) or 5 μM benomyl (B, E, and H), or 50 nM taxol (C, F, and I), fixed and processed to visualize the DLC and tubulin as described in Section 2. DLC (red), tubulin (green), and the merged images of the DLC staining (G, H, and I) are shown. Scale bar, 20 μm.

agents increased the translocation of p53 into the nucleus [22]. Since, microtubules serve as tracks for several motor proteins, which transport cell organelles like mitochondria, vesicles [47] and signaling molecules [48], the organization and dynamics of microtubules are very important for their functions. It has been proposed that a single motor protein can travel only a short distance over the microtubule after which it has more chances of falling off and the cargoes are carried to longer distances only if carried by multiple motors [49]. Since the peripheral microtubules are known to be highly dynamic in nature [50] the chances of the motor proteins falling off the microtubular track are fairly high. Hence, fewer molecules of the minus end directed motor protein dynein were observed in the control cells compared to the suppressed dynamic instability conditions wherein increased localization of dynein was observed in the peripheral microtubules (Fig. 8). Therefore, the data indicated that suppression of microtubule dynamics increased the association of dynein and microtubules; and dynein could travel longer distance in the stabilized microtubules track compared to the labile track of the control cells.

The overexpression of the proapoptotic protein bax and p21 suggested that benomyl activated p53 in MCF-7 cells. The increased translocation of p53 into the nucleus in 5 μM benomyl-treated cells indicated that the suppression of microtubule dynamics increases the interactions of p53 with microtubules and facilitates the transport of p53 into the nucleus. The findings together indicated that stable microtubules are necessary for transportation of p53 into the nucleus. This idea gained further support from the observation that high concentrations of benomyl that induced microtubule depolymerization inhibited the nuclear accumulation of p53 strongly even in the presence of cisplatin. In contrast, low concentration of benomyl caused a strong increase in the nuclear localization of p53 in the presence of cisplatin. Although p53 is shown to be transported into the nucleus through the dynein/dynamitin complex [23,24], it can bind to microtubules directly and it was shown to bind preferentially to polymerized microtubules than to tubulin dimers [24]. Therefore, it is quite possible that the binding of p53 to the stabilized microtubules in the presence of low concentration of benomyl might prevent its degradation;

however, its transport into the nucleus needs the dynein/dynamitin motor complex [23,24].

Although, benomyl at higher concentration did not increase the nuclear accumulation of p53, it strongly induced apoptosis (Fig. 3A and B) indicating that benomyl can induce apoptosis both by a p53 mediated pathway and by a p53 independent pathway. Previously, benomyl was shown to induce apoptosis through the Bcl2–bax pathway in HeLa cells, which have mutated nonfunctional p53 [15].

The evidence presented in the study is in agreement with the hypothesis that the stabilization of microtubules increases the translocation of p53 into the nucleus, while, the disruption of microtubules causes an inhibition in the nuclear accumulation of p53 [22]. Recent studies indicate that the antifungal drug griseofulvin has the potential to be used as an anticancer drug [25–27]. The discoveries that benomyl suppresses microtubule dynamics at its lower effective inhibitory concentration and increases the nuclear accumulation of p53 will be helpful to explore the anticancer potential of benomyl and its metabolite carbendazim.

Acknowledgements

The work is supported by Swarnajayanti Fellowship to D.P. by the DST, Government of India and a SRF to K.R. by CSIR, New Delhi. We thank CRNTS, IIT Bombay, for providing the LSCM facility.

REFERENCES

[1] Davidse LC. Benzimidazole fungicides—mechanism of action and biological impact. Annu Rev Phytopathol 1986;4:43–65.
[2] Kilmartin JV. Purification of yeast tubulin by self-assembly *in vitro*. Biochemistry 1981;20:3629–33.
[3] Sherman H, Culik R, Jackson RA. Reproduction, teratogenic, and mutagenic studies with benomyl. Toxicol Appl Pharmacol 1975;32:305–15.
[4] Richards KL, Anders KR, Nogales E, Schwartz K, Downing KH, Botstein D. Structure–function relationships in yeast tubulins. Mol Biol Cell 2000;11:1887–903.
[5] Jung MK, Wilder IB, Oakley BR. Amino acid alterations in the benA (beta-tubulin) gene of *Aspergillus nidulans* that confer benomyl resistance. Cell Motil Cytoskeleton 1992;22:170–4.
[6] Davidse LC, Flach W. Differential binding of methyl benzimidazol-2-yl carbamate to fungal tubulin as a mechanism of resistance to this antimitotic agent in mutant strains of *Aspergillus nidulans*. J Cell Biol 1977;72:174–93.
[7] Friedman PA, Platzer EG. Interaction of anthelmintic benzimidazoles and benzimidazole derivatives with bovine brain tubulin. Biochim Biophys Acta 1978;544:605–14.
[8] Friedman PA, Platzer EG. Interaction of anthelmintic benzimidazoles with *Ascaris suum* embryonic tubulin. Biochim Biophys Acta 1980;630:271–8.
[9] Downing KH. Structural basis for the interaction of tubulin with proteins and drugs that affect microtubule dynamics. Annu Rev Cell Dev Biol 2000;16:89–111.
[10] Gupta K, Panda D. Perturbation of microtubule polymerization by quercetin through tubulin binding: a novel mechanism of its antiproliferative activity. Biochemistry 2002;41:13029–38.
[11] Sassman SA, Lee LS, Bischoff M, Turco RF. Assessing N,N′-dibutylurea (DBU) formation in soils after application of *n*-butylisocyanate and benlate fungicides. J Agric Food Chem 2004;52:747–54.
[12] Garcia-Sánchez F, Aguilar-Gallardo A. Fluorimetric determination of the fungicide benomyl after solvolysis. Mikrochim Acta 1994;116:211–8.
[13] Davidse LC. Antimitotic activity of methyl benzimidazol-2-yl carbamate (MBC) in *Aspergillus nidulans*. Pestic Biochem Physiol 1973;3:317–25.
[14] Morinaga H, Yanase T, Nomura M, Okabe T, Goto K, Harada N, et al. A benzimidazole fungicide, benomyl, and its metabolite, carbendazim, induce aromatase activity in a human ovarian granulose-like tumor cell line (KGN). Endocrinology 2004;145:1860–9.
[15] Rathinasamy K, Panda D. Suppression of microtubule dynamics by benomyl decreases tension across kinetochore pairs and induces apoptosis in cancer cells. Eur J Biochem 2006;273:4114–28.
[16] Jordan MA, Wilson L. Microtubules as a target for anticancer drugs. Nat Rev Cancer 2004;4:253–65.
[17] Honore S, Pasquier E, Braguer D. Understanding microtubule dynamics for improved cancer therapy. Cell Mol Life Sci 2005;62:3039–56.
[18] Singh P, Rathinasamy K, Mohan R, Panda D. Microtubule assembly dynamics: an attractive target for anticancer drugs. IUBMB Life 2008;60:368–75.
[19] Jordan MA, Kamath K. How do microtubule-targeted drugs work? An overview. Curr Cancer Drug Targets 2007;7:730–42.
[20] Mohan R, Panda D. Kinetic stabilization of microtubule dynamics by estramustine is associated with tubulin acetylation, spindle abnormalities, and mitotic arrest. Cancer Res 2008;68:6181–9.
[21] Blagosklonny MV, Schulte TW, Nguyen P, Mimnaugh EG, Trepel J, Neckers L. Taxol induction of p21WAF1 and p53 requires c-raf-1. Cancer Res 1995;55:4623–6.
[22] Giannakakou P, Nakano M, Nicolaou KC, O'Brate A, Yu J, Blagosklonny MV, et al. Enhanced microtubule-dependent trafficking and p53 nuclear accumulation by suppression of microtubule dynamics. Proc Natl Acad Sci USA 2002;99:10855–60.
[23] Roth DM, Moseley GW, Glover D, Pouton CW, Jans DA. A microtubule-facilitated nuclear import pathway for cancer regulatory proteins. Traffic 2007;8:673–86.
[24] Giannakakou P, Sackett DL, Ward Y, Webster KR, Blagosklonny MV, Fojo T. p53 is associated with cellular microtubules and is transported to the nucleus by dynein. Nat Cell Biol 2000;2:709–17.
[25] Ho YS, Duh JS, Jeng JH, Wang YJ, Liang YC, Lin CH, et al. Griseofulvin potentiates antitumorigenesis effects of nocodazole through induction of apoptosis and G2/M cell cycle arrest in human colorectal cancer cells. Int J Cancer 2001;91:393–401.
[26] Panda D, Rathinasamy K, Santra MK, Wilson L. Kinetic suppression of microtubule dynamic instability by griseofulvin: implications for its possible use in the treatment of cancer. Proc Natl Acad Sci USA 2005;102:9878–83.
[27] Rebacz B, Larsen TO, Clausen MH, Ronnest MH, Loffler H, Ho AD, et al. Identification of griseofulvin as an inhibitor of centrosomal clustering in a phenotype-based screen. Cancer Res 2007;67:6342–50.
[28] Skehan P, Storeng R, Scudiero D, Monks A, McMahon J, Vistica D, et al. New colorimetric cytotoxicity assay for anticancer-drug screening. J Natl Cancer Inst 1990;82:1107–12.

[29] Suresh D, Balakrishna MS, Rathinasamy K, Panda D, Mague JT. Large-bite bis(phosphite) ligand containing mesocyclic thioether moieties: synthesis, reactivity, group 11 (Cu(I), Au(I)) metal complexes and anticancer activity studies on a human cervical cancer (HeLa) cell line. Dalton Trans 2008;2285–92.
[30] Scatena CD, Stewart ZA, Mays D, Tang LJ, Keefer CJ, Leach SD, et al. Mitotic phosphorylation of Bcl-2 during normal cell cycle progression and Taxol-induced growth arrest. J Biol Chem 1998;273:30777–84.
[31] Srivastava RK, Srivastava AR, Korsmeyer SJ, Nesterova M, Cho-Chung YS, Longo DL. Involvement of microtubules in the regulation of Bcl2 phosphorylation and apoptosis through cyclic AMP-dependent protein kinase. Mol Cell Biol 1998;18:3509–17.
[32] Joshi HC, Cleveland DW. Differential utilization of beta-tubulin isotypes in differentiating neurites. J Cell Biol 1989;109:663–73.
[33] Zhou J, Panda D, Landen JW, Wilson L, Joshi HC. Minor alteration of microtubule dynamics causes loss of tension across kinetochore pairs and activates the spindle checkpoint. J Biol Chem 2002;277: 17200–8.
[34] Bradford MM. A rapid and sensitive method for the quantitation of microgram quantities of protein utilizing the principle of protein–dye binding. Anal Biochem 1976;72:248–54.
[35] Jensen SO, Thompson LS, Harry EJ. Cell division in *Bacillus subtilis*: FtsZ and FtsA association is Z-ring independent, and FtsA is required for efficient midcell Z-Ring assembly. J Bacteriol 2005;187:6536–44.
[36] Skare JT, Ahmer BM, Seachord CL, Darveau RP, Postle K. Energy transduction between membranes. TonB, a cytoplasmic membrane protein, can be chemically cross-linked *in vivo* to the outer membrane receptor FepA. J Biol Chem 1993;268:16302–8.
[37] Kamath K, Jordan MA. Suppression of microtubule dynamics by epothilone B is associated with mitotic arrest. Cancer Res 2003;63:6026–31.
[38] Marcus AI, Zhou J, O'Brate A, Hamel E, Wong J, Nivens M, et al. The synergistic combination of the farnesyl transferase inhibitor lonafarnib and paclitaxel enhances tubulin acetylation and requires a functional tubulin deacetylase. Cancer Res 2005;65:3883–93.
[39] Desai A, Mitchison TJ. Microtubule polymerization dynamics. Annu Rev Cell Dev Biol 1997;13:83–117.
[40] Walker RA, O'Brien ET, Pryer NK, Soboeiro MF, Voter WA, Erickson HP, et al. Dynamic instability of individual, MAP-free microtubules analyzed by video light microscopy: rate constants and transition frequencies. J Cell Biol 1988;107:1437–48.
[41] Bulinski JC, Richards JE, Piperno G. Posttranslational modifications of α tubulin: detyrosination and acetylation differentiate populations of interphase microtubules in cultured cells. J Cell Biol 1988;106:1213–20.
[42] Piperno G, LeDizet M, Chang XJ. Microtubules containing acetylated α tubulin in mammalian cells in culture. J Cell Biol 1987;104:289–302.
[43] Jiang M, Yi X, Hsu S, Wang CY, Dong Z. Role of p53 in cisplatin-induced tubular cell apoptosis: dependence on p53 transcriptional activity. Am J Physiol Renal Physiol 2004;287:F1140–7.
[44] Maxwell SA, Ames SK, Sawai ET, Decker GL, Cook RG, Butel JS. Simian virus 40 large T antigen and p53 are microtubule-associated proteins in transformed cells. Cell Growth Differ 1991;2:115–27.
[45] Wilson PJ, Forer A. Effects of nanomolar taxol on crane-fly spermatocyte spindles indicate that acetylation of kinetochore microtubules can be used as a marker of poleward tubulin flux. Cell Motil Cytoskeleton 1997;37:20–32.
[46] Palazzo A, Ackerman B, Gundersen GG. Cell biology: tubulin acetylation and cell motility. Nature 2003;421:230.
[47] Schliwa M, Woehlke G. Molecular motors. Nature 2003;422:759–65.
[48] Gundersen GG, Cook TA. Microtubules and signal transduction. Curr Opin Cell Biol 1999;11:81–94.
[49] Gross A, Jockel J, Wei MC, Korsmeyer SJ. Enforced dimerization of BAX results in its translocation, mitochondrial dysfunction and apoptosis. EMBO J 1998;17:3878–85.
[50] Komarova YA, Vorobjev IA, Borisy GG. Life cycle of MTs: persistent growth in the cell interior, asymmetric transition frequencies and effects of the cell boundary. J Cell Sci 2002;115:3527–39.